Contents lists available at ScienceDirect

Nuclear Inst. and Methods in Physics Research B

Factors related to ^{41}K interference on ^{41}Ca AMS measurements

Carlos Vivo-Vilches[a,b,*], José María López-Gutiérrez[a,b], Manuel García-León[a,c], Christof Vockenhuber[d]

[a] Centro Nacional de Aceleradores (CNA) (Universidad de Sevilla, CSIC, Junta de Andalucía), Parque Científico y Tecnológico Cartuja, Thomas Alva Edison 7, 41092 Seville, Spain
[b] Dpto. de Física Aplicada I, Escuela Politécnica Superior, Universidad de Sevilla, Virgen de África 7, 41011 Seville, Spain
[c] Dpto. de Física Atómica Molecular y Nuclear, Universidad de Sevilla, Reina Mercedes s/n, 41012 Seville, Spain
[d] Laboratory of Ion Beam Physics, ETH-Zurich, Otto Stern Weg 5, 8093 Zurich, Switzerland

ABSTRACT

Dealing with the ^{41}K interference during ^{41}Ca measurement with low energy AMS systems is challenging. The detection of ^{39}K to correct the measured ^{41}Ca/^{40}Ca ratios is a powerful tool that improves precision and accuracy. However, the study of the sources of this interference can help to reduce it to its minimum.

In this work, it is shown that iron is a factor enhancing the production of the ^{41}K interference, since the (^{41}K^{57}Fe)$^-$ ion has the same mass as (^{41}K^{19}F$_3$)$^-$. To validate this observation, we measured ^{57}Fe^{2+} together with ^{41}M^{2+} (all ions with mass 41) and ^{39}K^{2+} in a blank sample and an aluminum target at the 600 kV AMS system at ETH Zurich.

We also show the temporal evolution of ^{41}M/^{40}Ca and ^{39}K/^{40}Ca ratios in two blank samples during a measurement on the 1 MV AMS system at CNA Seville. Even when unstable behavior for these ratios is observed for one of the blanks, the relationship between both, ^{41}M/^{39}K, is relatively stable over time. This supports the accuracy of the K–correction method, providing that it is applied sequence by sequence.

Two programs, one for each of these compact AMS systems, were written in FORTRAN code to deal with the complexity of the data analysis due to the K-correction.

1. Introduction

The main challenge during ^{41}Ca accelerator mass spectrometry (AMS) measurements is dealing with its stable isobar, ^{41}K. AMS systems based on accelerators with terminal voltages higher than 3 MV can minimize this interference using the different energy loss in different materials, such as silicon nitride foils or the counting gas from gas ionization chambers [1,2]. In compact AMS systems, with terminal voltages typically up to 1 MV, the energy straggling introduced by these materials is higher than the difference in the energy loss between both isobars [3,4].

Extracting (CaH$_3$)$^-$ from calcium hydride samples would be a solution because of the instability of (KH$_3$)$^-$ [5,6]. However, this compound is very hygroscopic and its handling is problematic. Consequently, this makes CaH$_2$ not suitable for ^{41}Ca AMS measurements when a large number of samples is involved.

The extraction of (CaF$_3$)$^-$ from calcium fluoride samples results in an increase the ^{41}K interference. Nevertheless, its simple chemical preparation is more suited for a large number of samples and CaF$_2$ is a chemically stable salt [5,7]. The ^{41}K/^{40}Ca interference is usually in the range of 10^{-11}.

This interference can be estimated by measuring the other stable isotope of potassium, ^{39}K (K-correction) [8]. To do this, the accelerator terminal and the electrostatic deflector voltages are changed sequentially, as is done, for instance, in actinides measurements [9,10]. The measured ^{41}K/^{39}K won't be exactly the terrestrial value, 0.07216, because of the slight differences in stripper and optical transmissions. To obtain the experimental ^{41}K/^{39}K, the relationship between the ^{39}K/^{40}Ca and ^{41}M/^{40}Ca (^{41}M denotes all ions with mass 41) ratios in blanks must be evaluated, since the relative contribution of the ^{41}K interference to the ^{41}M/^{40}Ca ratio will be more important for blanks than for samples with ^{41}Ca.

Until now, it was thought that, using this method, working with the 3 + state would not be possible because, during the counting of ^{39}K^{3+}, ^{13}C$^+$ ions would saturate the detector. Accordingly, charge state 2 + has been used, and relatively high stripper pressures have to be used to

---

destroy the molecular background. Because of this, the background due to scattering processes will be higher [11]. Recent studies at the 1 MV AMS system at CNA suggest that $^{13}C^+$ are not so high, and using the 3+ state could be possible.

With compact AMS systems it is not possible to independently identify ^{41}K, so it is important to understand the factors related to its production. During the first tests with CaF_2, theories suggested that $(KF_3)^-$ would be an unstable ion, and that ^{41}K would enter the accelerator as a different molecule but with the same mass as $(^{41}Ca^{19}F_3)^-$ [5]. Later studies demonstrated the existence of $(KF_3)^-$, in addition to other ions with the same mass, such as $(^{41}K^{57}Fe)^-$ [12].

We first present results relevant to this interference performed with two compact AMS systems: the 1 MV AMS system at CNA Seville (Spain) [13–15] and the 600 kV AMS system at ETH Zurich (Switzerland) [16–18]. The main goal is to demonstrate the existence of the $(K^{57}Fe)^-$ ion, and study its importance as an interfering species.

We then present the specifics of the K-correction as part of the data analysis of ^{41}Ca measurements with compact AMS systems.

2. ^{41}K interference: production and time evolution

2.1. Existence of the $(^{41}K^{57}Fe)^-$ ion and its relevance to ^{41}K interference

The existence of $(^{41}K^{19}F_3)^-$ does not imply that this would be the only molecular ion causing ^{41}K interference. Since $(^{41}K^{57}Fe)^-$ is a relatively simple ion with the same mass as $(^{41}K^{19}F_3)^-$, the presence of iron could be a relevant factor. The study from Ref. [12] observed that addition of iron to a calcium fluoride sample or sputtering stainless steel targets produced high ^{41}K rates.

The ^{41}K interference could be enhanced not just because $(^{41}K^{57}Fe)^-$ can be produced, but also because there can be a higher content of potassium in those materials. For example, some stainless steel materials have much higher trace amounts of potassium than copper [19]. In any case, there will be a small flux of K^+ ions implanting into a target as the Cs inevitably contains a degree of K impurity. The presence of Fe, whether or not it is accompanied by higher K content, is still a problem to avoid.

To prove that ^{57}Fe presence itself is a relevant factor involved in ^{41}K interference, a comparative experiment was performed with the 600 kV AMS system at ETH Zurich. Information about the ^{41}Ca measurements with this system has been published previously [3,8]. The first step was measuring $^{41}M^{2+}$ (^{41}M denotes all ions with mass 41) and $^{39}K^{2+}$ rates from a calcium fluoride blank sample (see Table 1 for target holder details) and a metallic aluminum target (Al-dummy). For this, the low energy side was tuned to inject masses 98 and 96. Afterwards, with the bouncer voltage of the low energy magnet selecting mass 96, the one from $(^{39}K^{19}F_3)^-$, the high energy sector was tuned to detect $^{57}Fe^{2+}$. Sputtering the Al-dummy, a rate > 1000 Hz was detected in the gas ionization chamber. We identified these ions as $^{57}Fe^{2+}$ by a process of elimination based on these observations:

- The count rate was independent of the stripper gas pressure. From this observation we infer that these were not molecular ions with mass 57 and charge state 2+.
- The signal in the detector was close in energy to that from $^{41}K^{2+}$ and $^{39}K^{2+}$, meaning that the energy was almost the same; it is likely that

the ion had a charge state of 2+.
- The odd-mass of ^{57}Fe precludes the presence of odd charge state ions with the same m/q ratio; $^{57}Fe^{2+}$ is the only ion of even charge state and mass lower than 96 with that m/q ratio.

As it can be seen in Table 1, $^{57}Fe^{2+}$ rates were much higher when sputtering the Al dummy than when sputtering the blank sample. Since ^{57}Fe was not measured sequentially with the potassium isotopes, only a qualitative comparison can be made. There is a proportional relationship between both potassium isotope rates and the $^{57}Fe^{2+}$ rate. Our observations also support the existence of $(KF_3)^-$, since F^+ was detected in both targets. The procedure to measure $^{19}F^+$ was equivalent to that for $^{57}Fe^{2+}$: tuning the bouncer voltage of the low energy magnet selecting mass 96, and the high energy for $^{19}F^+$. In this case, rates were much higher in the CaF_2 blank, as expected, saturating the detector. The relative contribution of ^{57}Fe to the K interference in CaF_2 samples, therefore, is negligible. However, this contribution will be higher when the target starts to run short of fluoride and the cathode and the pin are sputtered, or if the focusing of the Cs^+ ions to the sample is not optimal.

The influence of ^{57}Fe in the production of ^{41}K interference makes the choice of the material of the cathode holder relevant in reducing the interference. In Table 2 we present the average of the measured $^{39}K/^{40}Ca$ ratios in blank and standard samples pressed into different metal target holders: titanium, copper and aluminum. While there is no significant difference between titanium and copper, a slightly higher $^{39}K/^{40}Ca$ ratio was systematically found for the samples pressed into aluminum holders. This observation supports the role played by ^{57}Fe in the production of potassium ions, since aluminum is usually reported to have a higher trace content of iron than copper or titanium.

2.2. Time evolution of the ^{41}K interference

The high rates of potassium ions produced when metallic parts are sputtered lead to a strong variability of the ^{41}K interference in time. To characterize this, we have taken as an example the time evolution of several variables in two blank samples during one of our measurements in the 1 MV AMS system at CNA Seville. The performance parameters for ^{41}Ca measurement of this system have been recently published [4]. We selected a measurement where the output of the ion source was not optimal. Fig. 1 shows the evolution of 2 blank samples that displayed different behaviors. These data were collected from one of our routine sample measurements, so the sample was not continuously sputtered during 80 min, but in 10 different runs of 8 min each one.

Blank 1 presents a typical evolution of the $^{40}Ca^{2+}$ current: after a strong increase in the first 10 min, it keeps growing slowly until reaching its maximum after half an hour of sputtering, following which it starts decreasing smoothly. Because of the production of potassium isotopes by sputtering of the cathode holder, the decrease of the $^{40}Ca^{2+}$ current does not involve a decrease in $^{41}M^{2+}$ and $^{39}K^{2+}$ rates, which remain almost constant. Because of this, both $^{41}M/^{40}Ca$ and $^{39}K/^{40}Ca$ ratios are almost inversely related to the $^{40}Ca^{2+}$ current.

The $^{40}Ca^{2+}$ current behavior of blank 2 was more unstable: it strongly grew during the first 20 min, reaching a sharp maximum, after which it exponentially decreased. Since $^{41}M^{2+}$ and $^{39}K^{2+}$ increased 20 min longer, $^{41}M/^{40}Ca$ and $^{39}K/^{40}Ca$ had substantial increases. In this case, the $^{41}K/^{40}Ca$ interference reaches levels higher than 10^{-10}.

Table 1
Different ion rates in an aluminum target and a blank sample. The calcium fluoride blank was mixed with silver in a CaF_2:Ag weight ratio of 1:9 and pressed into a titanium target holder.

Target	$^{41}M^{2+}$ (s^{-1})	$^{39}K^{2+}$ (s^{-1})	$^{57}Fe^{2+}$ (s^{-1})	$^{19}F^{1+}$ (s^{-1})
Al dummy	1243 ± 63	16270 ± 550	1368 ± 95	460 ± 14
CaF_2 blank	143.4 ± 3.5	1402 ± 34	194 ± 29	> 10000

Table 2
$^{39}K/^{40}Ca$ ratios from standard and blank samples when different metals are used for the target holder.

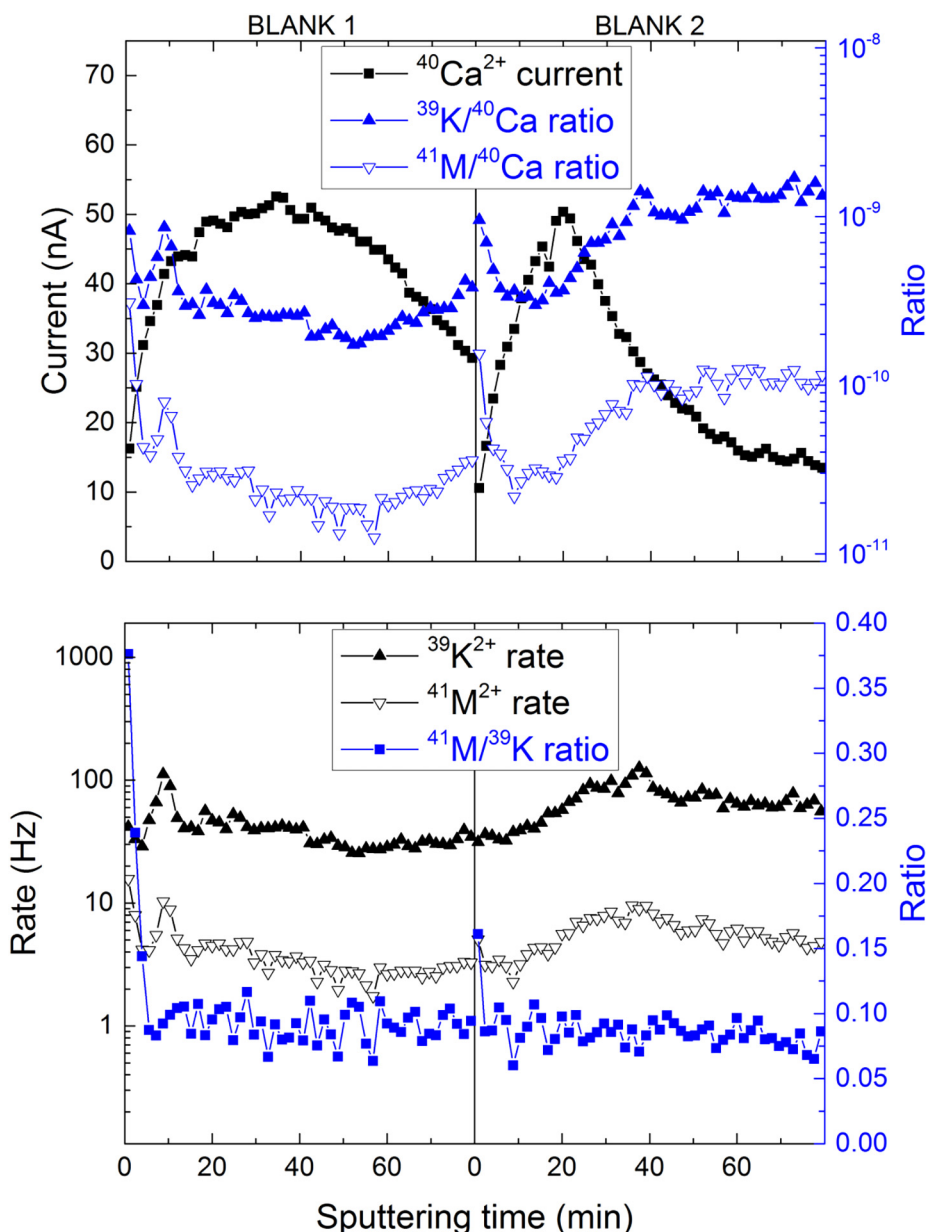| Target holder material	$^{39}K/^{40}Ca$
Titanium	$(5.5 ± 1.0) × 10^{-10}$
Copper	$(4.01 ± 0.72) × 10^{-10}$
Aluminum	$(9.05 ± 0.91) × 10^{-10}$

Fig. 1. Time evolution of the $^{41}M^{2+}$ and $^{39}K^{2+}$ rates; the ^{40}Ca current; and the $^{41}M/^{40}Ca$, $^{39}K/^{40}Ca$ and $^{41}M/^{39}K$ ratios in 2 blank samples during a measurement with the 1 MV AMS system at CNA Seville.

Since this huge difference is observed in 2 cathodes from the same blank material, it seems clear that treating the ^{41}K interference as part of the background is not advisable. On the other hand, even with the unstable behavior of blank 2, the $^{41}M/^{39}K$ ratio is pretty stable in both cases. The average value from this ratio is 0.092 ± 0.012 for blank 1, and 0.0843 ± 0.0096 for blank 2. This shows that the K-correction is a robust tool to estimate and correct the ^{41}K interference if it is applied sequentially, as it is explained in the next section.

In both cases, the first minutes of sputtering show more unstable behavior, so results from the first minutes of sputtering are not used during the data analysis. The correlation between the $^{39}K/^{40}Ca$ and $^{41}M/^{40}Ca$ in all the blanks used during this measurement can be seen in Fig. 2. After implementing the K-correction, a $^{41}Ca/^{40}Ca$ background of $(7.1 \pm 2.4) \times 10^{-12}$ was found.

3. Data analysis of ^{41}Ca AMS measurements at low energies

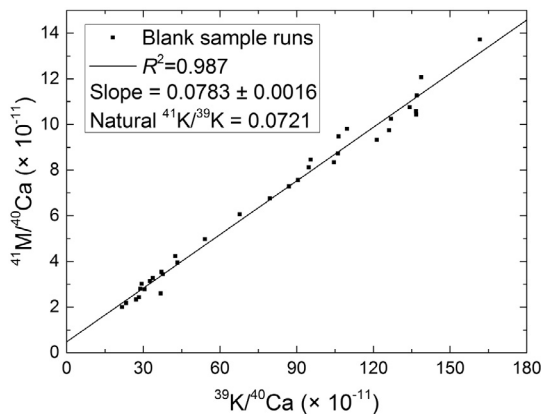A typical ^{41}Ca measurement procedure, including the detection ^{39}K,

Fig. 2. Linear correlation between $^{39}K/^{40}Ca$ and $^{41}M/^{40}Ca$ in 9 runs from 4 blank cathodes. The slope from this regression is used as the experimental $^{41}K/^{39}K$ ratio during the measurements.

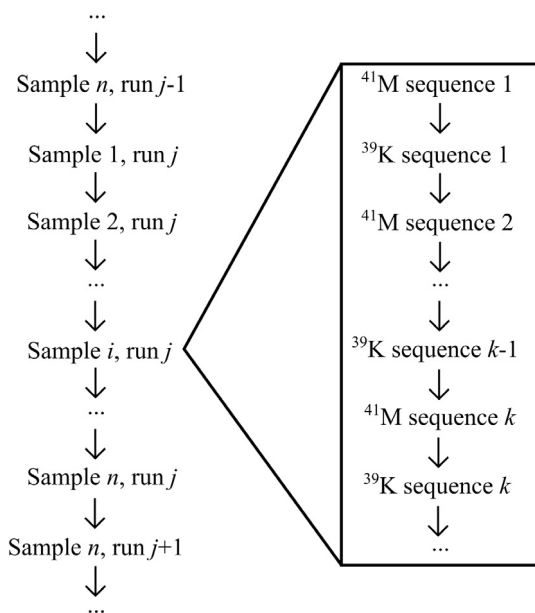**Fig. 3.** Measurement diagram for a ^{41}Ca measurement to implement K-correction.

Table 3

^{41}Ca/^{40}Ca of 3 different cathodes from the same sample, the ETH in-house standard B11, depending on how the ^{41}K background is treated. Nominal ratio from Ref. [20].

Cathode	Nominal ^{41}Ca/^{40}Ca ($\times 10^{-12}$)	^{41}Ca/^{40}Ca without K-correction ($\times 10^{-12}$)	^{41}Ca/^{40}Ca with K-correction ($\times 10^{-12}$)
B11A	41.60 ± 0.42	55 ± 14	44.2 ± 3.0
B11B		46 ± 15	41.7 ± 2.7
B11C		45.5 ± 9.4	43.1 ± 2.9

is shown in Fig. 3. *i* refers to a specific sample, while *j* denotes a specific run, and *k* denotes the specific sequence within that run. During the measurements on the 1 MV system at CNA we set a sequence time of 30 s for ^{41}M and 10 s for ^{39}K. Each run consist of 5 sequences for each of both masses. A transition time of 4 s is set between sequences to allow the accelerator terminal and electrostatic analyzer to settle.

^{41}K/^{40}Ca varies in time; therefore, to reduce the uncertainty, the K-correction is applied in each sequence before calculating average values. Since different mass ions will have slightly different stripper and optical transmissions, we need to determine the ^{41}K/^{39}K ratio that will be applied to estimate the ^{41}K/^{40}Ca interference from the ^{39}K/^{40}Ca ratio.

The first step of the K-correction is to calculate the preliminary average values of ^{41}M/^{40}Ca(i,j) and ^{39}K/^{40}Ca(i,j) for the blanks. Using ^{39}K/^{40}Ca(i,j) as the independent variable, and ^{41}M/^{40}Ca(i,j) as the dependent variable, we obtain the linear regression $y = \alpha \cdot x + \beta$. As shown in Fig. 2, α represents the measured ^{41}K/^{39}K ratio; the slope and its uncertainty are obtained using a least squares fit.

The second step is to apply this experimentally determined ^{41}K/^{39}K to all the samples, including standards and blanks, sequence by sequence. Since ^{39}K/^{40}Ca is not measured simultaneously with ^{41}M/^{40}Ca, but just before and after, the K-corrected ^{41}Ca/^{40}Ca from each sequence will be

$$R_{41,\text{K}-\text{corr}}(i,j,k) = R_{41}(i,j,k) - \alpha \cdot \frac{R_{39}(i,j,k-1) + R_{39}(i,j,k)}{2} \qquad (1)$$

where $R_{41,\text{K-corr}}$ denotes the K-corrected ^{41}Ca/^{40}Ca ratio; R_{41}, the uncorrected ^{41}M/^{40}Ca; and R_{39}, the ^{39}K/^{40}Ca ratio. The average of both measured ^{39}K/^{40}Ca ratios, before and after the (i,j,k) ^{41}M sequence, is used as the ^{39}K/^{40}Ca ratio during that sequence. The remainder of the procedure is common to other AMS measurements: obtaining the average K-corrected ^{41}Ca/^{40}Ca ratios for each sample *i*, calculating and subtracting the background, and normalizing the measurements to standards.

The K-correction adds some complexity to the data analysis. To optimize the analysis of the results, two programs were written in FORTRAN to perform all the data analysis: one for the measurements on the 1 MV system at CNA Seville, "caanalisiscna"; and another one for the measurements on the 600 kV system at ETH Zurich, "caanalisiseth". Both programs perform the analysis directly from the output files of the

data acquisition softwares.

Table 3 shows how the ^{41}Ca/^{40}Ca measured ratio of the ETH in-house ^{41}Ca standard B11 improves when the K-correction is used in one of the measurements with the 600 kV AMS system at ETH Zurich. If ^{41}K is treated as part of the background, relative uncertainties higher than 20% are obtained for this sample, and results differ substantially from the nominal value. The other 2 standards, B9 and B10, were used for the standard correction. The K-correction also reduced the ^{41}Ca/^{40}Ca background in that measurement from $(39.7 \pm 6.0) \times 10^{-12}$ to $(8.7 \pm 1.4) \times 10^{-12}$.

4. Conclusions

Although the $(\text{KF}_3)^-$ ion can be produced, and represents a source of background for the measurement of ^{41}Ca, the relatively high mass of the molecular ion $(\text{CaF}_3)^-$ allows injection of other molecules in which ^{41}K is present. This work proves the existence of $(^{41}\text{K}^{57}\text{Fe})^-$ and its enhancement of the ^{41}K interference. This makes iron a factor to take into account during the chemical preparation of the samples and loading into cathodes.

The production of ^{41}K from elements outside of the sample itself, such as the cathodes, causes the variability of the ^{41}K/^{40}Ca interference in time. In measurements with compact AMS systems, the measurement of ^{39}K to estimate the ^{41}K interference (K-correction) is the best option dealing with this background issue.

The variability along measurement time also implies that the K-correction has to be applied sequence by sequence. The development of computer programs for off-line data analysis is quite necessary, considering the addition of this relatively complex correction.

The possibility of performing ^{41}Ca AMS at low energy selecting the 3+ state and including the K-corrections is being studied at the 1 MV AMS system at CNA Seville.

References

[1] C. Vockenhuber, R. Golser, W. Kutschera, A. Priller, P. Steier, K. Vorderwinkler, A. Wallner, The ΔTOF detector for isobar separation at ion energies below 1 MeV/amu, Nucl. Instrum. Methods Phys. Res. Sect. B Beam Interact. Mater. Atoms 240 (2005) 490–494, http://dx.doi.org/10.1016/j.nimb.2005.06.169.

[2] S. Hosoya, K. Sasa, T. Matsunaka, T. Takahashi, M. Matsumura, H. Matsumura, M. Sundquist, M. Stodola, K. Sueki, Optimization of a ΔE-E detector for ^{41}Ca AMS, Nucl. Instrum. Methods Phys. Res. Sect. B Beam Interact. Mater. Atoms 406 (2017) 268–271, http://dx.doi.org/10.1016/j.nimb.2017.03.161.

[3] T. Schulze-König, C. Maden, E. Denk, S.P.H. Freeman, M. Stocker, M. Suter, H.-A. Synal, T. Walczyk, Comparison of ^{41}Ca analysis on 0.5 MV and 5 MV AMS systems, Nucl. Instrum. Methods Phys. Res. Sect. B Beam Interact. Mater. Atoms 268 (2010) 752–755, http://dx.doi.org/10.1016/j.nimb.2009.10.022.

[4] C. Vivo-Vilches, J.M. López-Gutiérrez, M. García-León, C. Vockenhuber, T. Walczyk, ^{41}Ca measurements on the 1 MV AMS facility at the Centro Nacional de

Aceleradores (CNA, Spain), Nucl. Instrum. Methods Phys. Res. Sect. B Beam Interact. Mater. Atoms 413 (2017) 13–18, http://dx.doi.org/10.1016/j.nimb.2017.10.003.

[5] D. Fink, R. Middleton, J. Klein, P. Sharma, ^{41}Ca: Measurement by accelerator mass spectrometry and applications, Nucl. Instrum. Methods Phys. Res. Sect. B Beam Interact. Mater. Atoms 47 (1990) 79–96, http://dx.doi.org/10.1016/0168-583X(90)90049-Z.

[6] A. Wallner, O. Forstner, R. Golser, G. Korschinek, W. Kutschera, A. Priller, P. Steier, C. Vockenhuber, Fluorides or hydrides? ^{41}Ca performance at VERA's 3 MV AMS facility, Nucl. Instrum. Methods Phys. Res. Sect. B Beam Interact. Mater. Atoms 268 (2010) 799–803, http://dx.doi.org/10.1016/j.nimb.2009.10.034.

[7] P.W. Kubik, D. Elmore, AMS of ^{41}Ca using the CaF$_3$ negative ion, Radiocarbon 31 (1989) 324–326, http://dx.doi.org/10.1017/S0033822200011863.

[8] C. Vockenhuber, T. Schulze-König, H.-A. Synal, I. Aeberli, M.B. Zimmermann, Efficient ^{41}Ca measurements for biomedical applications, Nucl. Instrum. Phys. Res. Sect. B Beam Interact. Mater. Atoms 361 (2015) 273–276, http://dx.doi.org/10.1016/j.nimb.2015.05.014.

[9] E. Chamizo, S.M. Enamorado, M. García-León, M. Suter, L. Wacker, Plutonium measurements on the 1 MV AMS system at the Centro Nacional de Aceleradores (CNA), Nucl. Instrum. Methods Phys. Res. Sect. B Beam Interact. Mater. Atoms 266 (2008) 4948–4954, http://dx.doi.org/10.1016/j.nimb.2008.08.001.

[10] L.K. Fifield, Accelerator mass spectrometry of the actinides, Quat. Geochronol. 3 (2008) 276–290, http://dx.doi.org/10.1016/j.quageo.2007.10.003.

[11] M. Suter, A new generation of small facilities for accelerator mass spectrometry, Nucl. Instrum. Methods Phys. Res. Sect. B Beam Interact. Mater. Atoms 139 (1998) 150–157, http://dx.doi.org/10.1016/S0168-583X(97)00945-2.

[12] X.-L. Zhao, J. Eliades, Q. Liu, W.E. Kieser, A.E. Litherland, S. Ye, L.M. Cousins, Studies of anions from sputtering III: the ^{41}K background in measurement by AMS, Nucl. Instrum. Methods Phys. Res. Sect. B Beam Interact. Mater. Atoms 268 (2010) 816–819, http://dx.doi.org/10.1016/j.nimb.2009.10.038.

[13] M. Klein, D.J.W. Mous, A. Gottdang, A compact 1 MV multi-element AMS system, Nucl. Instrum. Methods Phys. Res. Sect. B Beam Interact. Mater. Atoms 249 (2006) 764–767, http://dx.doi.org/10.1016/j.nimb.2006.03.135.

[14] E. Chamizo, F.J. Santos, J.M. López-Gutiérrez, S. Padilla, M. García-León, J. Heinemeier, C. Schnabel, G. Scognamiglio, Status report of the 1 MV AMS facility at the Centro Nacional de Aceleradores, Nucl. Instrum. Methods Phys. Res. Sect. B Beam Interact. Mater. Atoms 361 (2015) 13–19, http://dx.doi.org/10.1016/j.nimb.2015.02.022.

[15] G. Scognamiglio, E. Chamizo, J.M. López-Gutiérrez, A.M. Müller, S. Padilla, F.J. Santos, M. López-Lora, C. Vivo-Vilches, M. García-León, Recent developments of the 1 MV AMS facility at the Centro Nacional de Aceleradores, Nucl. Instrum. Methods Phys. Res. Sect. B Beam Interact. Mater. Atoms 375 (2016) 17–25, http://dx.doi.org/10.1016/j.nimb.2016.03.033.

[16] H.-A. Synal, S.A.W. Jacob, M. Suter, The PSI/ETH small radiocarbon dating system, Nucl. Instrum. Methods Phys. Res. Sect. B Beam Interact. Mater. Atoms 172 (2000) 1–7, http://dx.doi.org/10.1016/S0168-583X(00)00376-1.

[17] M. Stocker, R. Bertschinger, M. Döbeli, M. Grajcar, S.A.W. Jacob, J. Scheer, M. Suter, H.-A. Synal, Status of the PSI/ETH compact AMS facility, Nucl. Instrum. Methods Phys. Res. Sect. B Beam Interact. Mater. Atoms 223–224 (2004) 104–108, http://dx.doi.org/10.1016/j.nimb.2004.04.024.

[18] M. Stocker, M. Döbeli, M. Grajcar, M. Suter, H.-A. Synal, L. Wacker, A universal and competitive compact AMS facility, Nucl. Instrum. Methods Phys. Res. Sect. B Beam Interact. Mater. Atoms 240 (2005) 483–489, http://dx.doi.org/10.1016/j.nimb.2005.06.224.

[19] G. Rugel, S. Pavetich, S. Akhmadaliev, S.M. Enamorado Baez, A. Scharf, R. Ziegenrücker, S. Merchel, The first four years of the AMS-facility DREAMS: Status and developments for more accurate radionuclide data, Nucl. Instrum. Methods Phys. Res. Sect. B Beam Interact. Mater. Atoms 370 (2016) 94–100, http://dx.doi.org/10.1016/j.nimb.2016.01.012.

[20] M. Christl, C. Vockenhuber, P.W. Kubik, L. Wacker, J. Lachner, V. Alfimov, H.-A. Synal, The ETH Zurich AMS facilities: performance parameters and reference materials, Nucl. Instrum. Methods Phys. Res. Sect. B Beam Interact. Mater. Atoms 294 (2013) 29–38, http://dx.doi.org/10.1016/j.nimb.2012.03.004.